STRUCTURAL BIOLOGY COMMUNICATIONS

ISSN 2053-230X

Expression, purification, crystallization and X-ray diffraction studies of the molecular chaperone prefoldin from *Homo sapiens*

Yoshiki Aikawa, Hiroshi Kida, Yuichi Nishitani and Kunio Miki*

Department of Chemistry, Graduate School of Science, Kyoto University, Sakyo-ku, Kyoto 606-8502, Japan. *Correspondence e-mail: miki@kuchem.kyoto-u.ac.jp

Received 12 June 2015
Accepted 23 July 2015

Edited by A. Nakagawa, Osaka University, Japan

Keywords: protein folding; molecular chaperone; prefoldin.

Proper protein folding is an essential process for all organisms. Prefoldin (PFD) is a molecular chaperone that assists protein folding by delivering non-native proteins to group II chaperonin. A heterohexamer of eukaryotic PFD has been shown to specifically recognize and deliver non-native actin and tubulin to chaperonin-containing TCP-1 (CCT), but the mechanism of specific recognition is still unclear. To determine its crystal structure, recombinant human PFD was reconstituted, purified and crystallized. X-ray diffraction data were collected to 4.7 Å resolution. The crystals belonged to space group $P2_12_12$, with unit-cell parameters a = 123.2, b = 152.4, c = 105.9 Å.

1. Introduction

Proper protein folding is an essential process for all organisms. Several proteins require assistance by molecular chaperones to attain their native conformations (Hartl & Hayer-Hartl, 2002). Prefoldin (PFD), a molecular chaperone that is present in archaea and eukaryotes, facilitates the folding of non-native proteins by transferring them to group II chaperonin (Vainberg *et al.*, 1998). Crystal structures of archaeal PFD revealed a jellyfish-like structure with six coiled coils consisting of two α subunits and four β subunits (Siegert *et al.*, 2000; Ohtaki *et al.*, 2008; Kida *et al.*, 2008). It has been suggested that hydrophobic patches on the coiled-coil tentacles of archaeal PFD interact with various target proteins to prevent aggregation (Leroux *et al.*, 1999; Siegert *et al.*, 2000; Martín-Benito *et al.*, 2007; Ohtaki *et al.*, 2008). In contrast, eukaryotic PFD consists of six different subunits (PFD1–PFD6; Vainberg *et al.*, 1998). PFD3 and PFD5 are homologous to the archaeal α subunit, and the others are homologous to the β subunit. Eukaryotic PFD specifically recognizes nascent polypeptide chains of actin and tubulin, and delivers them to the chaperonin-containing TCP-1 (CCT), a eukaryotic group II chaperonin (Vainberg *et al.*, 1998; Hansen *et al.*, 1999). Although cryo-electron microscopy structures of PFD–actin and PFD–CCT complexes suggested a handoff mechanism for the delivery of non-native actin (Martín-Benito *et al.*, 2002), a higher resolution structure of eukaryotic PFD is necessary to elucidate how PFD recognizes non-native actin and tubulin. Here, we report the expression, purification, crystallization and preliminary X-ray diffraction studies of human PFD.

2. Materials and methods

2.1. Cloning and expression

The DNA fragment encoding each PFD subunit was amplified by PCR from a human liver cDNA library (Takara

Table 1
Macromolecule-production information.

The restriction sites used in the primer sequences and the hexahistidine tags removed by thrombin are underlined.

PFD1	
Source organism	*Homo sapiens*
DNA source	Human liver cDNA library
Forward primer	ATATCATATGGCCGCCCCCGTGGATCTAG
Reverse primer	CGGGATCCCTACTGGGCCCTTCGTGCCATCAG
Cloning vector	pET-21a
Expression vector	pET-21a
Expression host	*E. coli* Rosetta2 (DE3) pLysS
Complete amino-acid sequence of the construct produced	MAAPVDLELKKAFTELQAKVIDTQQKVKLADIQIEQLNRTKKHAHLTDTEIMTLVDETNMYEGVGRMFILQSKEAIHSQLLEKQKIAEEKIK-ELEQKKSYLERSVKEAEDNIREMLMARRAQ
PFD2	
Source organism	*H. sapiens*
DNA source	Human liver cDNA library
Forward primer	ATATCATATGGCGGAGAACAGCGGTCGC
Reverse primer	CGGGATCCCTAGGAGACCAACACTCCAGCTGAG
Cloning vector	pET-28a
Expression vector	pET-28a
Expression host	*E. coli* Rosetta2 (DE3) pLysS
Complete amino-acid sequence of the construct produced	MGSSHHHHHHSSGLVPRGSHMAENSGRAGKSSGSGAGKGAVSAEQVIAGFNRLRQEQRGLASKAAELEMELNEHSLVIDTLKEVDETRKCYR-MVGGVLVERTVKEVLPALENNKEQIQKIIETLTQQLQAKGKELNEFREKHNIRLMGEDEKPAAKENSEGAGAKASSAGVLVS
PFD3	
Source organism	*H. sapiens*
DNA source	Human liver cDNA library
Forward primer	GGAATTCCATATGAAACAGCCTGGGAATGAGACTGCAG
Reverse primer	CGGGATCCTTATGCTTTGTTCTTGGTAGAGTCATCCTTGTTTCTTC
Cloning vector	pET-21a
Expression vector	pET-21a
Expression host	*E. coli* Rosetta2 (DE3) pLysS
Complete amino-acid sequence of the construct produced	MKQPGNETADTVLKKLDEQYQKYKFMELNLAQKKRRLKGQIPEIKQTLEILKYMQKKKESTNSMETRFLLADNLYCKASVPPTDKVCLWLGA-NVMLEYDIDEAQALLEKNLSTATKNLDSLEEDLDFLRDQFTTTEVNMARVYNWDVKRRNKDDSTKNKA
PFD4	
Source organism	*H. sapiens*
DNA source	Human liver cDNA library
Forward primer	GGAATTCCATATGAAGAAGGCGGCTGCAGAAGATGTCAATG
Reverse primer	CGGGATCCTTAACTTTCATCAGCTTCAAGGTTTATGTTGCTCCCG
Cloning vector	pET-28a
Expression vector	pET-28a
Expression host	*E. coli* Rosetta2 (DE3) pLysS
Complete amino-acid sequence of the construct produced	MGSSHHHHHHSSGLVPRGSHMKKAAAEDVNVTFEDQQKINKFARNTSRITELKEEIEVKKKQLQNLEDACDDIMLADDDCLMIPYQIGDVFI-SHSQEETQEMLEEAKKNLQEEIDALESRVESIQRVLADLKVQLYAKFGSNINLEADES
PFD5	
Source organism	*H. sapiens*
DNA source	Human liver cDNA library
Forward primer	GGAATTCCATATGGCGCAGTCTATTAACATCACGGAGC
Reverse primer	CGGATCCTCAGGCCTTAGCAGTAGCCTGAG
Cloning vector	pET-21a
Expression vector	pET-21a
Expression host	*E. coli* Rosetta2 (DE3) pLysS
Complete amino-acid sequence of the construct produced	MAQSINITELNLPQLEMLKNQLDQEVEFLSTSIAQLKVVQTKYVEAKDCLNVLNKSNEGKELLVPLTSSMYVPGKLHDVEHVLIDVGTGYYV-EKTAEDAKDFFKRKIDFLTKQMEKIQPALQEKHAMKQAVMEMMSQKIQQLTALGAAQATAKA
PFD6	
Source organism	*H. sapiens*
DNA source	Human liver cDNA library
Forward primer	GGAATTCCATATGGCGGAGCTGATCCAGAAGAAGCTACAG
Reverse primer	GGGATCCCTCAGGCCTTGCCAGGAGCCCC
Cloning vector	pET-21a
Expression vector	pET-21a
Expression host	*E. coli* Rosetta2 (DE3) pLysS
Complete amino-acid sequence of the construct produced	MAELIQKKLQGEVEKYQQLQKDLSKSMSGRQKLEAQLTENNIVKEELALLDGSNVVFKLLGPVLVKQELGEARATVGKRLDYITAEIKRYES-QLRDLERQSEQQRETLAQLQQEFQRAQAAKAGAPGKA

Bio, Shiga, Japan) using the primers listed in Table 1. The N-terminal 37 residues of PFD3 and four residues of PFD4 were deleted. The fragments were individually cloned into the NdeI/BamHI sites of pET-21a (Novagen, Darmstadt, Germany) for PFD1, PFD3, PFD5 and PFD6 and of pET-28a for PFD2 and PFD4. The resulting sequences contained N-terminal hexahistidine tags followed by thrombin cleavage sites on PFD2 and PFD4. The plasmids for PFD1, PFD4, PFD5 and PFD6 were individually transformed into *Escherichia coli* Rosetta2 (DE3) pLysS cells (Novagen). The cells were grown to an OD_{600} of 0.6 in Luria–Bertani broth with appropriate antibiotics. Expression of these subunits was induced for 8 h at 293 K, for 4 h at 310 K, for 8 h at 293 K and for 2 h at 310 K, respectively, by adding 1 m*M* isopropyl β-D-1

thiogalactopyranoside. The plasmids for PFD2 and PFD3 were co-transformed into *E. coli* Rosetta2 (DE3) pLysS cells. Cell culture and induction of expression were carried out similarly with induction for 4 h at 310 K.

2.2. Purification

All purification steps were carried out at 277 K. Cells expressing PFD subunits were mixed and lysed by sonication in buffer *A* (50 m*M* sodium phosphate pH 7.0, 300 m*M* NaCl, 5 m*M* *β*-mercaptoethanol). For affinity purification using hexahistidine tags on PFD2 and PFD4, the supernatant was applied onto Talon Superflow Metal Affinity Resin (Clontech, California, USA) equilibrated with buffer *A*. The protein was eluted with buffer *A* containing 150 m*M* imidazole. This step excludes the mis-assembled specimens that carry no hexahistidine tags. The eluted sample was treated with thrombin for 16 h for tag removal, and was further purified using a Mono S cation-exchange column (GE Healthcare, Little Chalfont, England) by eluting with a linear gradient of 0.1–1 *M* NaCl in buffer *B* [20 m*M* 2-(*N*-morpholino)ethanesulfonic acid pH 6.0, 1 m*M* dithiothreitol (DTT)]. Finally, the sample was purified using a Superdex 200 10/300 gel-filtration column (GE Healthcare) equilibrated with buffer *C* (20 m*M* Tris–HCl pH 7.5, 150 m*M* NaCl, 1 m*M* DTT). The purity of the sample was confirmed by SDS–PAGE followed by Coomassie staining (Fig. 1*a*). The band pattern of the sample was similar to that previously reported for bovine PFD (Vainberg *et al.*, 1998), suggesting the successful reconstitution and purification of recombinant human PFD.

2.3. SEC-MALS

The molecular mass of purified PFD was determined by size-exclusion chromatography with multi-angle light scattering (SEC-MALS) using a Superdex 200 10/300 column connected to a miniDAWN detector (Wyatt Technology, California, USA; Fig. 1*b*). The purified sample was diluted to 0.5 mg ml^{-1} in buffer *D* (100 m*M* Tris–HCl pH 7.5, 300 m*M* NaCl). A 100 µl aliquot was loaded onto the column and eluted with buffer *D* at a flow rate of 0.5 ml min^{-1}. The signal at a 90° angle was analyzed using the *Astra* software (Wyatt Technology). The average molecular masses of the first and

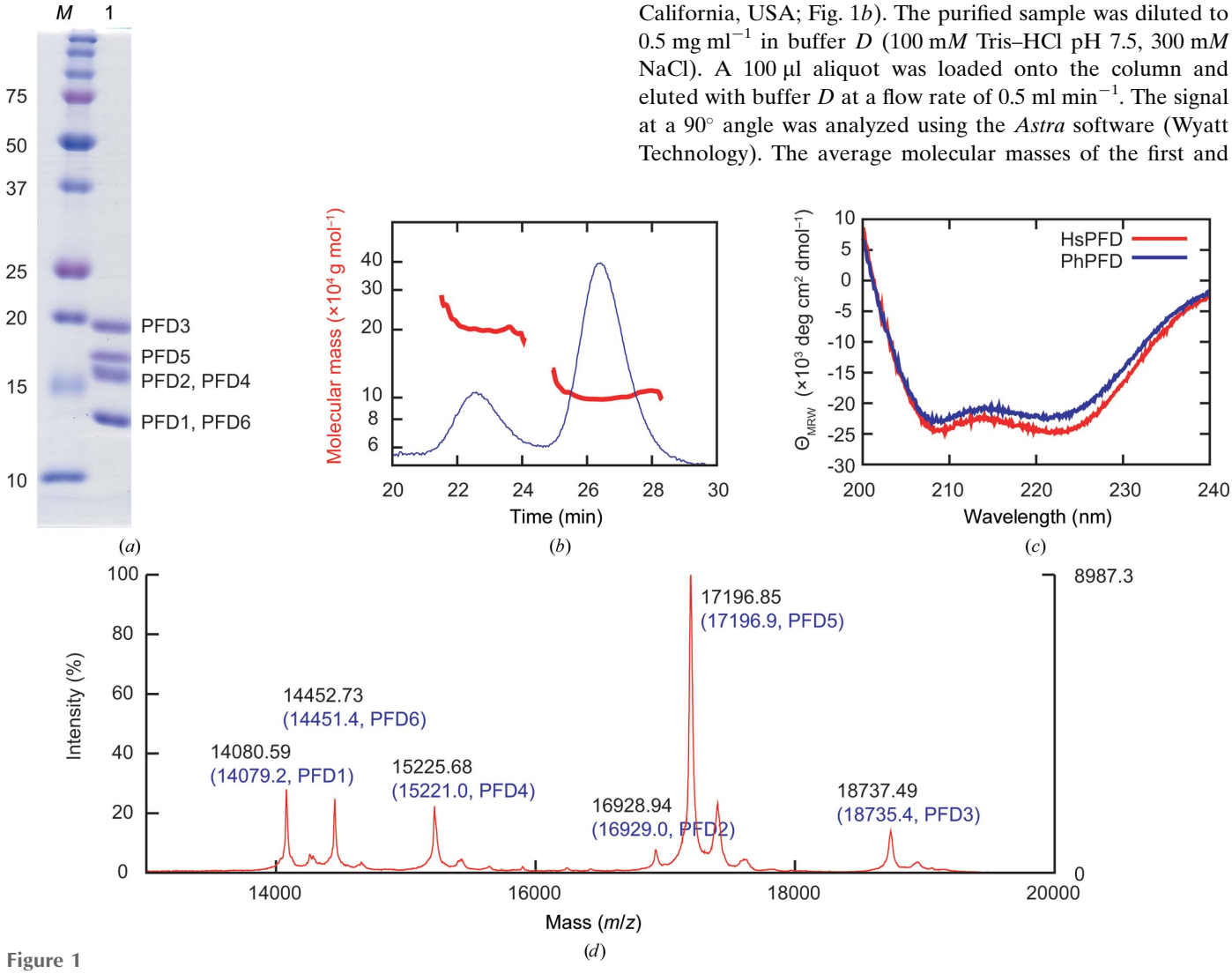

Figure 1
Biochemical characterization of human PFD. (*a*) SDS–PAGE analysis of purified human PFD. Lane *M*, molecular-weight marker (labelled in kDa); lane 1, peak fraction from Superdex 200 column. PFD subunits are assigned to the bands according to the molecular weights calculated from the sequences. (*b*) SEC-MALS of purified PFD. Red, molecular mass; blue, absorbance at 280 nm. (*c*) CD spectra. Red, spectrum of human PFD (HsPFD); blue, spectrum of *P. horikoshii* PFD (PhPFD). (*d*) MALDI-TOF MS. Peaks are annotated with the observed molecular mass (black) and the calculated mass from the sequence (blue, in parentheses).

second peaks were 204.8 and 100.6 kDa, corresponding to a dimer and a monomer of hexameric PFD (97.0 kDa), respectively. Although dimerization of PFD was also observed, this result supports the proper reconstitution of recombinant PFD.

2.4. CD spectroscopy

Circular-dichroism (CD) spectra of PFD were measured in a quartz cuvette with a path length of 1 mm using a J-805 spectropolarimeter (Jasco, Tokyo, Japan) at 298 K (Fig. 1*c*). Protein samples were diluted to 0.1 mg ml^{-1} in buffer *E* (10 m*M* Tris–HCl pH 7.5, 1 m*M* DTT) before measurements. The buffer baseline was subtracted from the spectra and five scans were averaged. The mean residue molar ellipticities ($\Theta_{\rm MRW}$) were calculated using the equation

$$\Theta_{\rm MRW} = \Theta/10ncl,$$

where n is the number of amino-acid residues, c is the molar concentration and l is the path length. The secondary structure of human PFD consisted of 79% α-helix and 21% β-sheet. The spectrum of human PFD was similar to that of the archaeal jellyfish-like PFD from *Pyrococcus horikoshii* (PhPFD; Ohtaki *et al.*, 2008). These results suggest that human PFD has a jellyfish-like structure similar to that of PhPFD.

2.5. MALDI-TOF MS

To confirm the correct assembly of PFD subunits, matrix-assisted laser desorption/ionization time-of-flight mass spectrometry (MALDI-TOF MS) was performed (Fig. 1*d*). Sinapinic acid was dissolved at 10 mg ml^{-1} in 0.1% TFA and 50% acetonitrile. PFD was diluted to 10 pmol ml^{-1} and mixed with the sinapinic acid solution. The mixed solution was spotted onto a MALDI plate and the solvents were vaporized. Mass calibration was carried out using apo myoglobin (16.95 kDa) and cytochrome *c* (12.36 kDa). The mass spectrum showed peaks corresponding to all six subunits of PFD, suggesting the correct assembly of PFD. The molecular masses of PFD1, PFD5 and PFD6 were ∼131 Da lower than those calculated from the sequences, respectively. We interpret these results as the deletion of the N-terminal methionines during expression in *E. coli*.

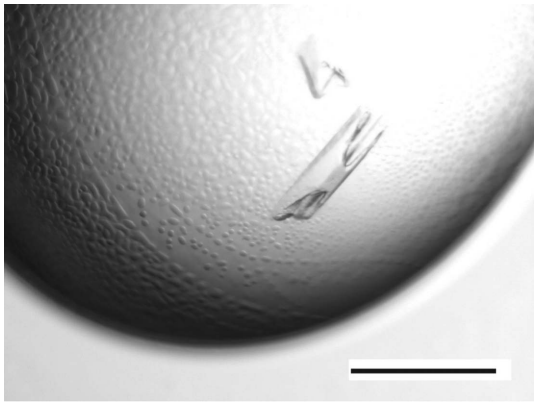

Figure 2
Crystals of human PFD. The black bar represents 0.5 mm.

2.6. Crystallization

Initial screening for crystallization condition was carried out at 293 K by the sitting-drop vapour-diffusion method using several commercial screening kits. Each crystallization drop was prepared by mixing equal volumes (0.3 µl each) of protein solution (10 mg ml^{-1} in 20 m*M* Tris–HCl pH 7.5, 1 m*M* DTT) and reservoir solution and equilibrating against 60 µl reservoir solution. Crystals were obtained in one condition with a reservoir consisting of 100 m*M* Tris–HCl pH 8.5, 9.9%(*v*/*v*) 2-propanol, 9.9%(*w*/*v*) polyethylene glycol (PEG) 3350. After optimizing the condition, crystals suitable for diffraction experiments were obtained by the hanging-drop vapour-diffusion method. Equal volumes (1.5 µl each) of protein solution (7.5 mg ml^{-1} in 10 m*M* Tris–HCl pH 7.5, 1 m*M* DTT) and reservoir solution [100 m*M* Tris–HCl pH 8.6, 11%(*w*/*v*) PEG 3350] were mixed and equilibrated against 500 µl reservoir solution at 293 K. Crystals with approximate dimensions of 300 × 100 × 20 µm were obtained within one week (Fig. 2).

2.7. X-ray data collection

The crystals were soaked in reservoir solution supplemented with 20%(*w*/*v*) PEG 4000 and flash-cooled in a nitrogen-gas stream at 95 K. X-ray diffraction data were collected on beamline BL1A at the Photon Factory, Tsukuba, Japan using a Pilatus 2M-F detector (Dectris, Baden, Swit-

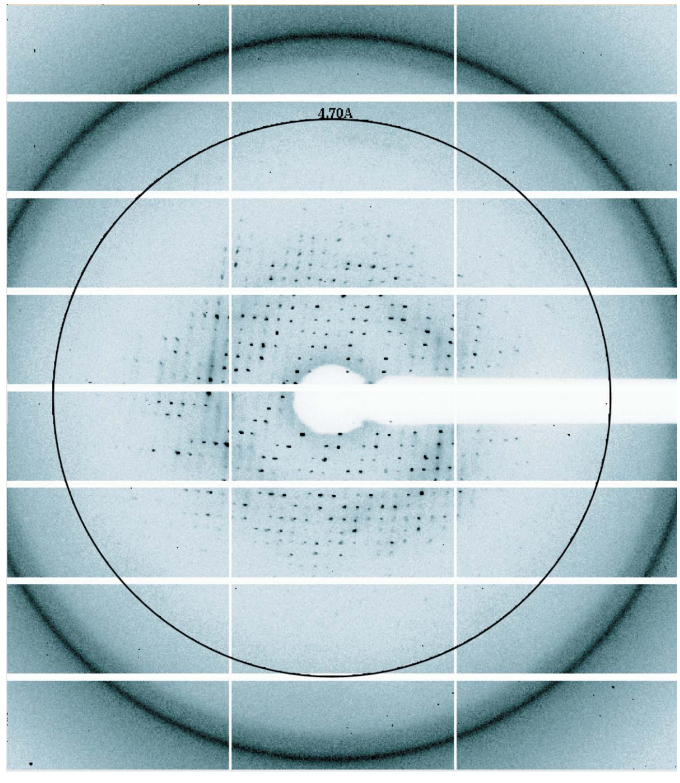

Figure 3
X-ray diffraction pattern from a crystal of human PFD. The circle represents 4.7 Å resolution.

Table 2
Data-collection statistics for a crystal of human PFD.

Values in parentheses are for the highest resolution shell.

Diffraction source	BL1A, Photon Factory
Wavelength (Å)	1.1
Temperature (K)	95
Detector	Pilatus 2M-F
Crystal-to-detector distance (mm)	440
Rotation range per image (°)	1
Total rotation range (°)	180
Exposure time per image (s)	0.5
Space group	$P2_12_12$
a, b, c (Å)	123.2, 152.4, 105.9
Mosaicity (°)	0.87–3.40
Resolution range (Å)	50–4.7 (4.87–4.70)
Total No. of reflections	52378
No. of unique reflections	10172
Completeness (%)	92.9 (88.1)
Multiplicity	5.2 (4.0)
$\langle I/\sigma(I)\rangle$	22.7 (2.3)
$R_{\rm p.i.m.}$† (%)	3.0 (30.5)

† $R_{\rm p.i.m.} = \sum_{hkl}\{1/[N(hkl)-1]\}^{1/2}\sum_i |I_i(hkl) - \langle I(hkl)\rangle|/\sum_{hkl}\sum_i I_i(hkl)$, where $I_i(hkl)$ is the ith intensity measurement of reflection hkl, $\langle I(hkl)\rangle$ is the mean intensity for this reflection and $N(hkl)$ is the multiplicity.

zerland; Fig. 3) and on BL41XU at SPring-8, Harima, Japan using a MX225HE detector (Rayonix, Illinois, USA). A data set consisting of 180 frames was collected with an oscillation angle of 1° per frame. The data set was processed and scaled with the *HKL*-2000 package (Otwinowski & Minor, 1997). The data-collection statistics are summarized in Table 2.

3. Results and discussion

Recombinant human PFD was reconstituted and purified from an *E. coli* expression system. SDS–PAGE, SEC-MALS and MALDI-TOF MS analyses suggested successful reconstitution and purification of heterohexameric PFD. A CD spectroscopic study suggested that human PFD has a jellyfish-like structure similar to those of its archaeal homologues. Crystals of human PFD were obtained using PEG 3350 as the main precipitant. X-ray diffraction data were indexed and scaled at 4.7 Å resolution. The crystals belonged to space group $P2_12_12$, with unit-cell parameters a = 123.2, b = 152.4, c = 105.9 Å. Assuming the presence of two PFD hexamers in the asymmetric unit, the Matthews coefficient ($V_{\rm M}$) and solvent content were calculated to be 2.5 Å^3 Da^{-1} and 50.2%, respectively (Matthews, 1968).

Acknowledgements

The authors are grateful to the beamline staff at Photon Factory and SPring-8 for their assistance during data collection. The authors are also grateful to Dr Masafumi Yohda for providing purified PhPFD. The diffraction experiment was performed on beamlines BL1A at the Photon Factory with the approval of KEK (Proposal No. 2013G659) and BL41XU at SPring-8 with the approval of the Japan Synchrotron Radiation Research Institute (JASRI; Proposal Nos. 2007A1829, 2009B1694, 2011A1602, 2011B1672 and 2012A1704). This work was supported by a grant from the National Project on Protein Structural and Functional Analyses (to KM) and from the Global COE Program 'Integrated Material Science' (No. B-024) of the Ministry of Education, Culture, Sports, Science and Technology (MEXT) of Japan (to YA and HK).

References

Hansen, W. J., Cowan, N. J. & Welch, W. J. (1999). *J. Cell Biol.* **145**, 265–277.
Hartl, F. U. & Hayer-Hartl, M. (2002). *Science*, **295**, 1852–1858.
Kida, H., Sugano, Y., Iizuka, R., Fujihashi, M., Yohda, M. & Miki, K. (2008). *J. Mol. Biol.* **383**, 465–474.
Leroux, M. R., Fändrich, M., Klunker, D., Siegers, K., Lupas, A. N., Brown, J. R., Schiebel, E., Dobson, C. M. & Hartl, F. U. (1999). *EMBO J.* **18**, 6730–6743.
Martín-Benito, J., Boskovic, J., Gómez-Puertas, P., Carrascosa, J. L., Simons, C. T., Lewis, S. A., Bartolini, F., Cowan, N. J. & Valpuesta, J. M. (2002). *EMBO J.* **21**, 6377–6386.
Martín-Benito, J., Gómez-Reino, J., Stirling, P. C., Lundin, V. F., Gómez-Puertas, P., Boskovic, J., Chacón, P., Fernández, J. J., Berenguer, J., Leroux, M. R. & Valpuesta, J. M. (2007). *Structure*, **15**, 101–110.
Matthews, B. W. (1968). *J. Mol. Biol.* **33**, 491–497.
Ohtaki, A., Kida, H., Miyata, Y., Ide, N., Yonezawa, A., Arakawa, T., Iizuka, R., Noguchi, K., Kita, A., Odaka, M., Miki, K. & Yohda, M. (2008). *J. Mol. Biol.* **376**, 1130–1141.
Otwinowski, Z. & Minor, W. (1997). *Methods Enzymol.* **276**, 307–326.
Siegert, R., Leroux, M. R., Scheufler, C., Hartl, F. U. & Moarefi, I. (2000). *Cell*, **103**, 621–632.
Vainberg, I. E., Lewis, S. A., Rommelaere, H., Ampe, C., Vandekerckhove, J., Klein, H. L. & Cowan, N. J. (1998). *Cell*, **93**, 863–873.